

## Influence of deep-pits on the device characteristics of metal-organic chemical vapor deposition grown AlGaN/GaN high-electron mobility transistors on silicon substrate

S. Lawrence Selvaraj, Arata Watanabe, and Takashi Egawa

Citation: *Appl. Phys. Lett.* **98**, 252105 (2011); doi: 10.1063/1.3602919

View online: <http://dx.doi.org/10.1063/1.3602919>

View Table of Contents: <http://apl.aip.org/resource/1/APPLAB/v98/i25>

Published by the American Institute of Physics.

### Related Articles

Gate traps inducing band-bending fluctuations on AlGaN/GaN heterojunction transistors  
*Appl. Phys. Lett.* **102**, 023511 (2013)

Novel metal gates for high  $\kappa$  applications  
*J. Appl. Phys.* **113**, 034107 (2013)

Organic field-effect transistor nonvolatile memories based on hybrid nano-floating-gate  
*Appl. Phys. Lett.* **102**, 023303 (2013)

Organic field-effect transistor nonvolatile memories based on hybrid nano-floating-gate  
*APL: Org. Electron. Photonics* **6**, 11 (2013)

Fast and slow transient charging in various III-V field-effect transistors with atomic-layer-deposited-Al<sub>2</sub>O<sub>3</sub> gate dielectric  
*Appl. Phys. Lett.* **102**, 022104 (2013)

### Additional information on *Appl. Phys. Lett.*

Journal Homepage: <http://apl.aip.org/>

Journal Information: [http://apl.aip.org/about/about\\_the\\_journal](http://apl.aip.org/about/about_the_journal)

Top downloads: [http://apl.aip.org/features/most\\_downloaded](http://apl.aip.org/features/most_downloaded)

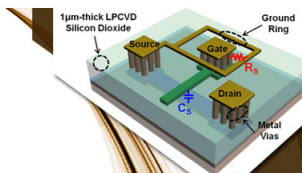
Information for Authors: <http://apl.aip.org/authors>

## ADVERTISEMENT



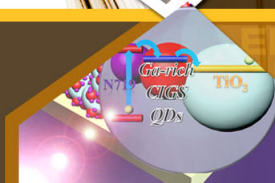
**EXPLORE WHAT'S  
NEW IN APL**

**SUBMIT YOUR PAPER NOW!**



### **SURFACES AND INTERFACES**

Focusing on physical, chemical, biological, structural, optical, magnetic and electrical properties of surfaces and interfaces, and more...



### **ENERGY CONVERSION AND STORAGE**

Focusing on all aspects of static and dynamic energy conversion, energy storage, photovoltaics, solar fuels, batteries, capacitors, thermoelectrics, and more...

# Influence of deep-pits on the device characteristics of metal-organic chemical vapor deposition grown AlGaN/GaN high-electron mobility transistors on silicon substrate

S. Lawrence Selvaraj,<sup>a)</sup> Arata Watanabe, and Takashi Egawa

Research Center for Nano-Device and System, Nagoya Institute of Technology, Gokiso-cho, Showa-ku, Nagoya 466-8555, Japan

(Received 22 April 2011; accepted 2 June 2011; published online 21 June 2011)

We have investigated the regions around deep-pits and their limitations on the performance of metal-organic chemical vapor deposition grown AlGaN/GaN high-electron-mobility transistors (HEMTs) on Si. The device characteristics such as maximum drain current density ( $I_{DSmax}$ ), threshold voltage ( $V_{th}$ ), and three terminal-OFF breakdown ( $BV_{OFF}$ ) of a HEMT were affected based on the distance of deep-pits from a device active region. The deterioration of HEMT characteristics are significant if the active region is present within 50  $\mu\text{m}$  radius of a deep-pit and becomes insignificant for distance beyond 50  $\mu\text{m}$ . These device characteristics were compared with optical measurements and it was found the region around 50  $\mu\text{m}$  radius of a pit have large dislocations and defects as confirmed by cathodoluminescence. Further, the  $E_2$  Raman shift measurements reveal additional stress in the 50  $\mu\text{m}$  region around a pit. © 2011 American Institute of Physics. [doi:10.1063/1.3602919]

AlGaN/GaN high-electron-mobility transistors (HEMTs) are attractive for high-power switching device applications. Among the available substrates (SiC, Sapphire, and Si), Si is the most suitable choice for epitaxial growth due to its large size availability and low cost. The advantage with Si is that it offers growth on large diameter substrate up to a size of 200 mm, which is not possible using either SiC or sapphire. However, the limiting factor for the growth of GaN on Si is the large lattice and thermal mismatches, which lead to large density of dislocations resulting in wafer bowing and cracking.

Apart from these common issues before GaN growth on Si, another important issue which needs investigation is the presence of hexagonal shaped deep-pits on the surface of the growth completed wafer. Earlier, we reported the nature of these pits and their impact on the three terminal-OFF breakdown ( $BV_{OFF}$ ).<sup>1</sup> These pits originate from the Si substrate and are present until the top AlGaN surface layer irrespective of using buffers of various thicknesses. It is difficult to grow pit-free structures on Si as the best grown wafers still have few deep-pits. Some of the grown wafers have very low density of deep pits and if HEMTs are fabricated on such wafers, the pits are found either within or outside the device active region (between source and drain). It is therefore necessary to study the detrimental effect of these pits on the device characteristics with relevant to their distance from the active region. In other way, we have to investigate the influential area of these pits that interferes with normal device operation of a HEMT. Identifying this influential region is important for avoiding the same during device fabrication to demonstrate ideal power and reliability characteristics. Therefore, in the current study, we selected samples, which have low pit density (830  $\text{cm}^{-2}$ ) and investigated the influence of these pits on the HEMT characteristics such as

$I_{DSmax}$ ,  $V_{th}$ , and  $BV_{OFF}$  with respect to distance from the active region of a HEMT. Further, these electrical characteristics were compared with optical measurements, namely, cathodoluminescence (CL) and Raman spectra measured at various distances from a deep-pit. Analyzing electrical and optical characteristics of deep-pits revealed more about its nature and the significant region around a pit affected by high dislocations and increased strain.

AlGaN/GaN HEMT heterostructures were grown using Taiyo-Nippon Sanso SR4000 horizontal metal-organic chemical vapor deposition (MOCVD) reactor. The current HEMT epilayers were grown on 4 in. Si starting with 100 nm AlN followed by 40 nm AlGaN, 4.0  $\mu\text{m}$  thick superlattice structure (SLS) buffer, 1  $\mu\text{m}$  i-GaN, and final 25 nm top  $\text{Al}_{0.26}\text{Ga}_{0.74}\text{N}$  layer. The density of deep-pits on these structures was calculated as 830  $\text{cm}^{-2}$  using Nomarski microscope image. In Fig. 1, the cross-sectional transmission electron microscope image shows pit size of 1.5  $\mu\text{m}$  diameter originating from the Si substrate. The v-shaped defect present throughout the grown epilayer starting from Si until the surface layer, as it can be seen from Fig. 1(a). A more clear view of SLS buffer at v-shaped defect is shown in Fig. 1(b). These pits originate from the Si substrate as shown in Fig. 1(c). HEMT devices passivated with 100 nm  $\text{SiO}_2$  were fabricated with dimensions of gate width ( $W_g$ ) = 15  $\mu\text{m}$ , gate length ( $L_g$ ) = 1.5  $\mu\text{m}$ , and gate-drain length ( $L_{gd}$ ) = 4  $\mu\text{m}$ . The process details of the HEMT fabrication are similar to our earlier letter.<sup>2</sup> The dc current-voltage ( $I_{DS}$ - $V_{DS}$ ) characteristics of the HEMTs were measured using Agilent 4156 semiconductor parameter analyzer. Since the pit density is low (<830  $\text{cm}^{-2}$ ), only one or two pits were present in the vicinity of the device region. A number of devices were carefully chosen in two categories, namely, (i) devices which had pit within the source-drain active region and (ii) devices which had pits outside active region. In both cases, nearest distance ( $d$ ) of the gate finger was calculated from a pit. All these HEMTs showed good pinchoff characteristics irrespec-

<sup>a)</sup> Author to whom correspondence should be addressed. Electronic mail: sselvaraj@yahoo.com. FAX: +81-52-7355546.

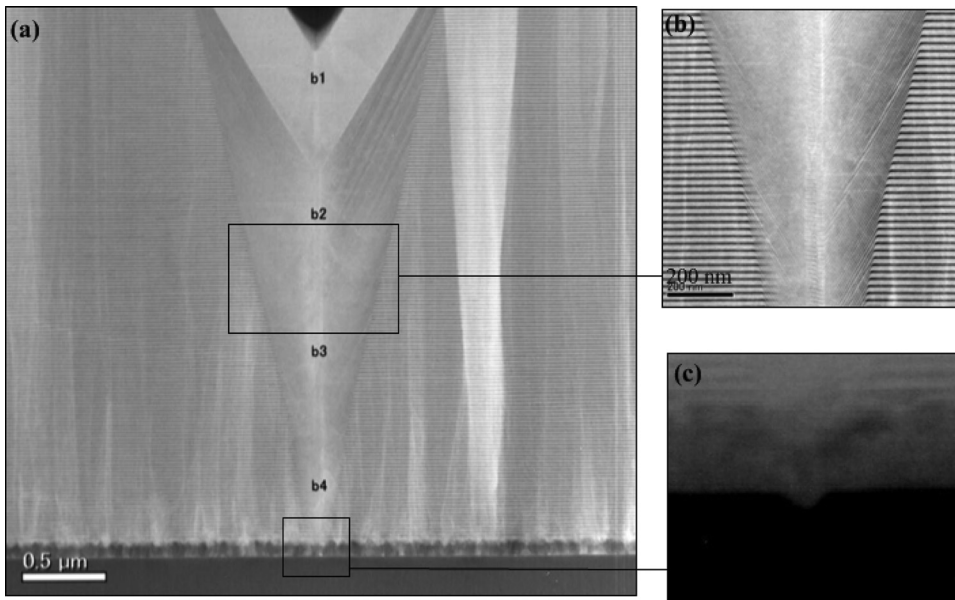


FIG. 1. (a) Cross-sectional transmission electron microscope image of AlGaN/GaN grown on Si substrate; (b) magnified view of the SLS buffer at v-shaped defect; (c) origin of the pit from Si substrate.

tive of the position of pit. However, there was a difference in the  $I_{DSmax}$  observed with regard to the position of these pits from active region. Figure 2 summarizes the  $I_{DSmax}$  observed for HEMTs with respect to pit at a distance. The HEMTs showed better  $I_{DSmax}$  when pits are beyond 50  $\mu\text{m}$  away from the device active region. However, 19% reduction in  $I_{DSmax}$  was observed when a pit is found within the active region as shown in Fig. 2. Further, this reduction in the  $I_{DSmax}$  were accompanied by a shift in the threshold voltage. HEMTs which had pit far away ( $d > 50 \mu\text{m}$ ) underwent complete pinchoff at  $-2.2 \text{ V}$ , whereas HEMTs which had pit near active region ( $d < 10 \mu\text{m}$ ) showed a positive shift in  $V_{th}$  causing an early pinchoff at  $-1.8 \text{ V}$ . This positive shift in  $V_{th}$  for HEMTs having pit within or near the active region signifies that dislocation densities are high around the region of a pit. Because it is known that dislocations in III-V nitride heterostructures can produce acceptorlike trap states,<sup>3,4</sup> which become negatively charged.<sup>5</sup> Therefore, for HEMTs located near the pit, high dislocations around the pit act as trapping centers for electrons in the two-dimensional electron gas (2DEG) channel. This results in partial depletion of 2DEG at the AlGaN/GaN interface causing a low  $I_{DSmax}$  and a positive  $V_{th}$  shift.

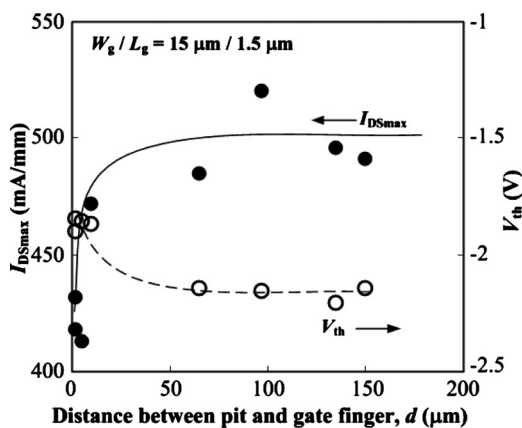


FIG. 2.  $I_{DSmax}$  (solid circle) and  $V_{th}$  (open circle) measured for HEMTs having pits at various distances ( $d$ ) from the gate terminal.

The three terminal-OFF breakdown measured on these devices remain unaffected when these pits are 50  $\mu\text{m}$  away from the active region. A drastic 50% reduction in the breakdown with high buffer and substrate leakage was observed when pits are found within the active region as summarized in Fig. 3. We reported that growing a thick buffer for the growth of GaN on Si restricts the buffer and substrate leakage causing a high breakdown.<sup>6</sup> However, in these samples with deep-pits, in spite of using a 4  $\mu\text{m}$  thick buffer, the presence of deep-pits causes high buffer and substrate leakage thus deteriorating the breakdown to a large extent. Therefore, the position of these deep-pits found to affect the device performances especially when they are within a short range ( $d < 50 \mu\text{m}$ ) from the active region. Hence, it is necessary to further study the quality of the GaN around 50  $\mu\text{m}$  radius of a deep-pit for further understanding.

In order to investigate the region around pits, CL was measured in a Hitachi SU-70 scanning electron microscope (SEM) using an Oxford instruments MonoCL4 system. After confirming the position of a pit with the help of SEM, CL was measured at various distances from the pit. The normalized CL spectra as in Fig. 4 show the band edge emission

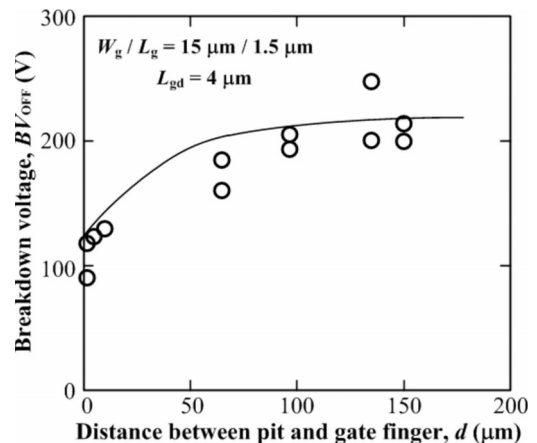


FIG. 3. Three terminal OFF-breakdown ( $BV_{OFF}$ ) measured for HEMTs having pits at various distances ( $d$ ) from the gate terminal;  $BV_{OFF}$  defined as  $V_{DS}$  at which a leakage of 1 mA/mm was observed.



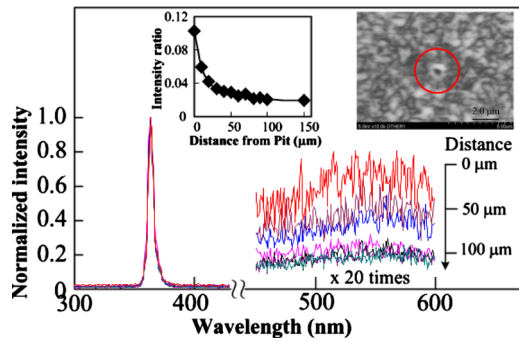


FIG. 4. (Color online) CL measured for an AlGaIn/GaN epilayer having pit. The CL was recorded by focusing the beam spot at various distances from a pit. Inset: intensity ratio ( $I_{Yel}/I_{Edge}$ ) decreased as CL was measured at a farther distance from a deep-pit, and a CL image captured around a deep-pit marked by a circle.

( $I_{Edge}$ ) at 364 nm corresponding to GaN band gap (3.4 eV). At wavelengths around 550 nm, yellow luminescence ( $I_{Yel}$ ) with varying peak intensity was observed for intensity measured at various distances from the pit. The intensity of yellow band emission depends on the growth conditions<sup>7</sup> and reflects the quality, unintentional doping of the GaN grown. A highest  $I_{Yel}$  was observed for CL measured at the pit and it gradually became weak as the beam spot moved away from the pit. The relative intensity ratio ( $I_{Yel}/I_{Edge}$ ), as in the inset of Fig. 4 shows a decrease in intensity ratio with increase in the distance from the pit. For CL measured at distances beyond 50  $\mu\text{m}$  from the pit, there is not much change in the intensity ratio. This illustrates that yellow luminescence is high for regions within 50  $\mu\text{m}$  of the deep-pits signifying a larger dislocation density for regions around deep-pits. The inset of Fig. 4 shows a CL image captured around a deep-pit.

In order to study the stress created by deep-pits, we performed micro-Raman measurements in  $E_2$  Raman mode, which is known to be shifted by stress alone.<sup>8</sup> To start with,  $E_2$  Raman spectra was measured on GaN substrate (shift at 567.6  $\text{cm}^{-1}$ ), which is considered as the reference (dashed line in Fig. 5) for unstressed GaN films. Then for samples with deep-pits, micro-Raman measurements were measured starting at the pit and at various distances from the pit. Before measurement it was confirmed that no other pits were present in the neighboring vicinity of 300  $\mu\text{m}$  radius of the pit chosen for investigation. The Raman shift peak position measured at various distances from the pit are shown in Fig. 5. Comparing with the peak position for unstressed GaN films, the  $E_2$  mode observed for our GaN on Si substrate confirms the presence of tensile stress.<sup>8</sup> It is well known that the type of stress observed for GaN grown on Si and sapphire is tensile and compressive, respectively. From Fig. 5, it is concluded that there is an additional tensile stress for regions within the 40  $\mu\text{m}$  range of a deep-pit. However, as we move away from the pit (beyond 40  $\mu\text{m}$ ), the Raman shift peak position remained constant without any additional

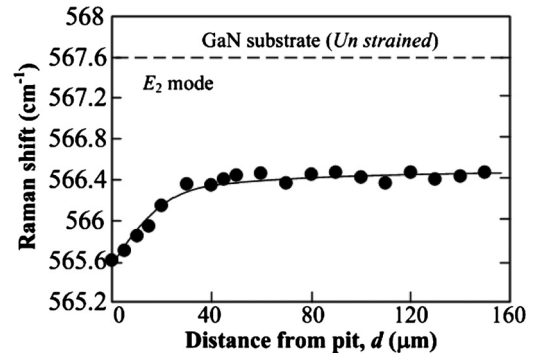


FIG. 5.  $E_2$  Raman shift measured at various distances from a pit. The  $E_2$  Raman shift peak position for a GaN substrate is identified with a dashed line.

change in tensile stress. This further confirms that regions beyond 50  $\mu\text{m}$  from a deep-pit do not pose any detrimental effects on the device performance.

As a summary, we have made an in-depth study on the regions around deep-pits and their limitations on the performance of MOCVD grown AlGaIn/GaN HEMTs on Si substrate. It is concluded that for regions within 50  $\mu\text{m}$  distance of deep-pits, there is a degradation observed in device performance. If the active region of the HEMTs are within the 50  $\mu\text{m}$  distance from a deep-pit, then it leads to 19% decrease in the  $I_{DSmax}$  and positive shift in the  $V_{th}$  signifying an early pinchoff. The early pinchoff for devices within the 50  $\mu\text{m}$  distance of deep-pit confirms the presence of high dislocations causing dislocation scattering. These high dislocations cause 50% decrease in  $BV_{OFF}$  due to large buffer and substrate leakage current. Further, the 50  $\mu\text{m}$  radius defective region around the pits was confirmed by CL and Raman shift measurements. Therefore, for AlGaIn/GaN epilayers grown on Si having a low density of deep-pits on the surface, the pits does not impede the normal performance of the HEMTs if the source/drain active region is located far away at a distance of 50  $\mu\text{m}$  from the deep-pits.

We thank Professor K. Fujita for the useful discussions.

<sup>1</sup>S. L. Selvaraj, T. Suzue, and T. Egawa, *Appl. Phys. Express* **2**, 111005 (2009).

<sup>2</sup>S. L. Selvaraj and T. Egawa, *Appl. Phys. Lett.* **89**, 193508 (2006).

<sup>3</sup>F. A. Ponce, D. P. Bour, W. Götz, and P. J. Wright, *Appl. Phys. Lett.* **68**, 57 (1996).

<sup>4</sup>D. M. Schaadt, E. J. Miller, E. T. Yu, and J. M. Redwing, *Appl. Phys. Lett.* **78**, 88 (2001).

<sup>5</sup>P. J. Hansen, Y. E. Strausser, A. N. Erickson, E. J. Tarsa, P. Kozodoy, E. G. Brazel, J. P. Ibbetson, U. Mishra, V. Narayanamurti, S. P. DenBaars, and J. S. Speck, *Appl. Phys. Lett.* **72**, 2247 (1998).

<sup>6</sup>S. L. Selvaraj, T. Suzue, and T. Egawa, *IEEE Electron Device Lett.* **30**, 587 (2009).

<sup>7</sup>T. Ogino and M. Aoki, *Jpn. J. Appl. Phys.* **19**, 2395 (1980).

<sup>8</sup>C. Kisielowski, J. Krüger, S. Ruvimov, T. Suski, J. W. Ager III, E. Jones, Z. L. Weber, M. Rubin, E. R. Weber, M. D. Bremser, and R. F. Davis, *Phys. Rev. B* **54**, 17745 (1996).